INDUCED AND SPONTANEOUS FISSION OF NOBELIUM ISOTOPES USING COLLECTIVE CLUSTERIZATION APPROACH

A thesis submitted in partial fulfilment of the requirements for the award of the degree of

Master of Science

In

Physics

Submitted by

JYOTI

Reg. No. 301504018

Under the supervision of

DR. MANOJ K. SHARMA

School of Physics and Materials Science

Thapar University, Patiala-147004, India

July-2017

I dedicate this thesis to my Parents who have always been supportive towards me.

CERTIFICATE

I hereby certify that the work which has been presented in this thesis entitled " **Induced and spontaneous fission of Nobelium isotopes using collective clusterization approach"** submitted by **Jyoti** for partial fulfilment of the requirements for the award of degree **of Master of Science in Physics** at **Thapar Institute of Engineering and Technology University, Patiala,** is an authentic record of my own work carried out under the supervision of **Dr. Manoj K. Sharma, Professor and Head, SPMS** and refers other researcher's work which are duly listed in reference section. The matter embodied in this thesis has not been submitted for the award of any other degree of this or any other university.

Jyoti

Date: 02-08-2017 **(Jyoti)**

This is to certify that the above statement made by the candidate is correct and true to best of my knowledge.

Dr. Manoj K. Sharma
Professor and Head of department
School of Physics and Materials Science
Thapar Institute of Engineering and Technology University
Patiala.

ACKNOWLEDGEMENT

I am using this opportunity to express my gratitude to everyone who supported me throughout this research work. I sincerely thankful and with a deep sense of gratitude to my supervisor, **Dr. Manoj K. Sharma, Professor and Head of department, SPMS** for his immense help in planning and executing the work in time. Without him this thesis is not possible. I thank him for his patience and encouragement. For me it is a matter of pride and pleasure to have a worked with him. His valuable suggestions as final words during the course of work are greatly acknowledged. My heartiest thanks to him for the help extended to me when I approached him and the valuable discussion during this thesis work.

I would like to express my heartiest gratitude to **Ms. Amandeep Kaur** research scholar for extending timely help in carrying out my important works out for her busy schedule. I also want to thank all the faculty members for their support and encouragement.

I am thankful to GOD, for always being there for me. I also want to thank my family for their support and blessings. I also want to thank to my friends and all those people who help me completing my thesis in time.

CONTENTS

List of Tables/ Figures

Table 3.1: Comparison of PCM calculated spontaneous fission half-lives ($T_{1/2}$) with experimental ones. The other related observables like neck-length parameter (ΔR), preformation probability P_0, penetrability P and assault frequency ν_0 are also presented.

ABSTRACT

The spontaneous fission (SF) has crucial importance in the identification and stability of numerous heavy and superheavy elements. In the recent years, various attempts have been made to investigate the dynamics of spontaneous fission from both the theoretical and experimental point of view. Here, in the present dissertation, I intend to analyze the properties of spontaneous fission decay of 'Nobelium' isotopes with mass varying from A=250 to 262. The performed cluster-decay model (PCM) based on quantum mechanical fragmentation theory (QMFT) is used to calculate the spontaneous fission half-lives ($T_{1/2}$). The calculated SF half-lives find reasonable agreement with the recent experimental data. The behaviour of fragment mass distributions for each spontaneous fissioning nuclei is investigated, which changes from asymmetric to symmetric with increment in the mass of parent nucleus. The most probable decaying fragments are identified, and are found to lie in the neighbourhood of the magic shell closures. Moreover, the spontaneous fission dynamics is explored by studying the fragmentation potential (V), preformation probability (P_0), barrier penetration probability (P) and total kinetic energy (TKE) corresponding to most preferred decaying fragments. In addition to this, a comparative analysis of SF and induced fission (fusion-fission) is carried out in terms of barrier characteristics and potential energy surfaces. Both the fission processes show similar behaviour with respect to fragment mass distribution. The 'barrier modification' effects have been explored and the requirement of barrier modification comes out to be relatively smaller for spontaneous fission as comparison to the induced fission process.

Chapter 1

Literature Review

1.1 Introduction

Nuclear physics is a branch of physics, focused to understand the properties of atomic nucleus, and the complete interactions among nucleons (protons and neutrons). In 1911, Ernest Rutherford discovered that an atom consists of a small dense core called nucleus and carries charge with electrons revolving around it. After its discovery, various attempts have been made to understand the mechanism behind the nuclear reactions and investigate the properties of nuclear matter. The main applications of nuclear physics are nuclear medicine, energy production, radio carbon dating and nuclear weapons etc. At present, 118 chemical elements are identified, of which the first 92 occur naturally and remaining 26 being synthetic elements. Moreover, the isotopes of element with $Z>83$ are exclusively radioactive, which decay with time to get the stable state. Nuclear stability represents a balance between two forces inside the nucleus, the strong nuclear forces and the Coulomb forces. Coulomb force comes into picture due to repulsion between two protons because of the same charge. If the number of protons present in the nucleus increase then Coulomb repulsion forces also increase, which in turn causes nuclear instability. The nuclear stability can be measured by the proportion of (N/Z), where N and Z is neutron number and atomic number present in the nucleus respectively. From figure 1.1 we can see that, for lighter atomic nuclides up to $Z=20$, the neutron to proton ratio is 1:1, which indicates the stability of such nuclei. As the atomic number starts increasing, the N/Z ratio also shows the increment until it is around 1.5:1 for very heavy systems. This is because the nuclei with higher number of protons need more neutrons to compensate the repulsive interaction due between the positively charged protons. The atomic nuclei which lie below and above the stability curve represented as shaded area in figure 1.1, are radioactive in nature. These unstable radioactive elements decay mainly via α, β and γ emission [1]. Apart from above decays there are three other ground state decays such as spontaneous fission (SF) [2], cluster radioactivity [3] and heavy particle radioactivity (HPR) [4].

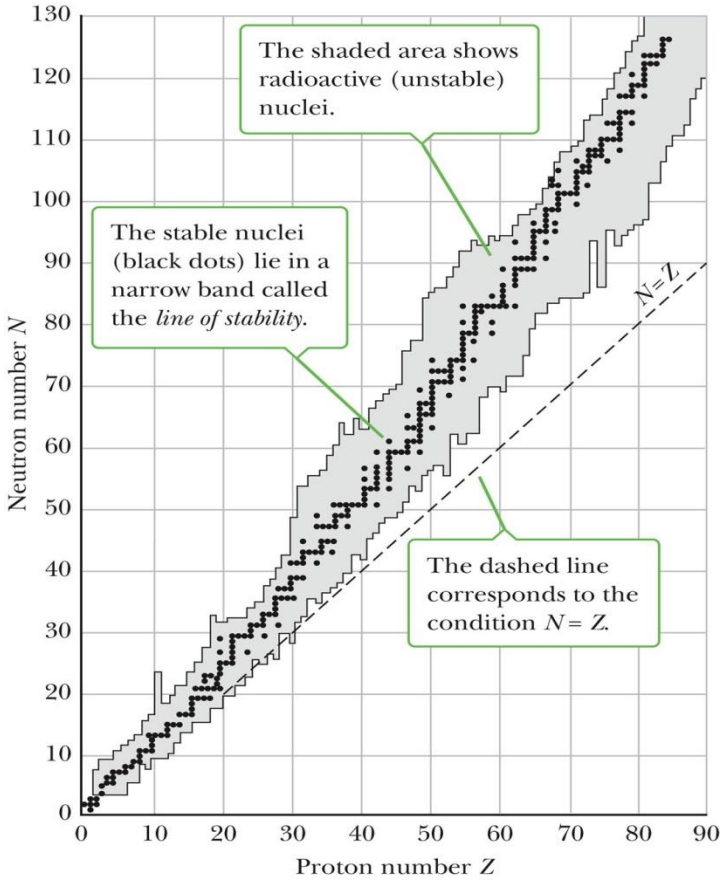

Figure 1.1: *Figure shows the curve between number of protons and neutrons. Shaded area depicts the radioactive nuclei and black dots represent the line of stability.*

Beside the ground state emissions, the nuclear reactions play very important role to understand the nuclear dynamics involved. The low energy (E≤15 MeV/nucleons) nuclear physics mainly focus on the phenomena such as fusion, fission, particle evaporation, quasi-fission etc. In a nuclear reaction, when the projectile and target nucleus amalgamate completely, they form a composite system which is statistically equilibrated in all degree of freedom. Depending upon its mass, the compound nucleus (CN) may decay through various decay modes like evaporation residue and fusion-fission.

The main motive of this work is to understand the decay of nuclear system via fission. On the basis of energy state, nuclear fission can be of two types: (i) ground state nuclear fission i.e. spontaneous fission (SF) and (ii) fission of excited compound nucleus induced by lighter or heavy ions. Nuclear fission firstly discovered [5] in 1938, by two chemists Otto Hahn and Fritz

Strassman, when they hit a neutron on Uranium nucleus, it split into two fragments Barium and Lanthanum. Later, in 1940, Flerov et al. [2] were the first to observe the process of spontaneous fission from Uranium nucleus. In order to study the different type of decay modes a variety of nuclear models are developed during last over seven decades. Here in the present work, for ground state decay the performed cluster-decay model (PCM) and for excited state decay the dynamical cluster decay model (DCM) is used, details are discussed in chapter 2. Both the models are based on quantum mechanical fragmentation theory (QMFT) [6]. The advantage of using such methodology is that it gives the relative probability of all fragments and hence the decay channels in the framework of collective clusterization approach.

1.2 Types of nuclear decay

There are mainly two types of nuclear decay: ground state and excited state decay. In the ground state emission, a parent nucleus decays without any influence of external source. On the other hand, in the excited state decay process, an energetic projectile hit on the target nucleus and form excited unstable compound nucleus (CN) which get stabilized by decaying into light particles or heavier fragments. A brief description of these mechanisms is discussed in the following sections.

1.3 Ground state decay

A radioactive nucleus does not have enough binding energy to hold the nucleus together and tend to attain stability by decaying through various channels such as α, β and γ decay. Apart from this, the emission of heavier cluster and fission fragments is also observed. After decaying some particles/clusters, the parent nucleus gets transformed into new element and this new element is called daughter nucleus.

1.3.1 Radioactivity (α, β and γ emission)

Radioactivity is a spontaneous process in which unstable nuclei emit some kind of radiations. It is discovered by Henri Bacqueral in 1896 [7], he observed that Uranium salt emits radiations which can penetrate a piece of paper. He performed a number of experiments using Uranium and photographic plate, and observed that some radiations are emitted from Uranium which inturn effected the photographic plate. According to the law of radiactivity “The rate of radioactive

decay of unstable element at any time (t) is directly proportional to the number of nucleons present in that radioactive nucleus". Let us consider N_0 be the total number of nucleons present in the radioactive element at time t=0 and N be the no. of nucleons present after time't'. Consider dN/dt is the rate of change of number of nucleons. According to law of disintegration

$$dN/dt = - \lambda N(t) .$$

Integrating both sides with respect to 't', we get

$$N(t) = N_0 e^{-\lambda t}$$

This equation depicts the exponential decay of radioactive elements. If we consider $N(t)=N_0/2$ at time 't' then above equation becomes

$$T_{1/2}=\ln(2)/ \lambda$$

This expression shows that half life is reciprocal of decay constant λ. Therefore, half life of a radioactive substance is defined as the interval in which the quantity of radioactive substance decreases to half of its original value. Hence, the half-life time is a tool for experimental and theoretical people to understand the ground state phenomenon and related nuclear stability aspects. After the discovery of Bacqueral, Rutherford [8] and Villiard [9] found that radiactivite radiations are divided into three types: α, β and γ which are discussed in briefly in next paragraph.

Alpha decay is a type of radioactive decay in which an unstable nucleus emits an α-particle and new daughter nucleus. Mass number of daughter nuclei is reduced by four and an atomic number by two from the parent nuclei. It usually occurs in heavy nuclei, due to quantum mechanical tunnelling of α-particle across the potential barrier. For example, ^{238}U decays to form ^{234}Th and emits α-particle. It is observed that alpha decay is the dominant decay mode in heavy and superheavy mass region. The newly synthesized superheavy nuclei generally decay via sequential α-emission. The energy range of such emitted α-particles depends on the half life of considering parent nuclei. The nuclei with long half-life emit less energy and vice versa. Most of the alpha particles carry energy between 2 MeV to 7 MeV. Apart from the above, if the radioactive element has either too many protons or neutrons then it undergoes the β-emission process. Beta decay is of two types (a) positive β-decay and (b) negative β-decay. Positive β-decay releases a positively charged β- particle (a positron) and a neutrino. On the contrary negative β-decay process occurs, when an electron is emitted in the company of an antineutrino.

The another important ground state decay mode is γ-emission, during which the unstable nucleus changes from a excited state to ground state through the emission of photons or electromagnetic radiation. The number of nucleons present in the radioactive system remains same and hence there is no formation of new element.

1.3.2 Cluster decay and heavy particle radioactivity (HPR)

The decay process in which radioactive nuclei emit fragments heavier than alpha particle (Z>2) but much smaller than the fission fragments is known as cluster radioactivity. Cluster decay usually happens in trans-lead and trans-tin region. In trans-lead region the non-alpha clusters like ^{14}C, $^{18,20}O$, ^{23}F, $^{24,26}Ne$, $^{28,30}Mg$ and ^{34}Si show the maximum probability of formation and hence smaller half lives in comparison to their neighbours. The $^{34}Si_{14}$ is highest cluster observed yet. Like α-decay mechanism, cluster decay [10] is also a quantum mechanical tunnelling process.

Moreover, when nucleus emits fragments which are much larger than α-particles but smaller than fragments emitted through nuclear fission, this type of radioactive process is known as heavy particle radioactivity (HPR) [11,12]. It is observed that the fragments decaying via HPR are much closer to the fission fragments. HPR generally emit clusters having $Z \geq 28$ and daughter nuclei is around magic nuclei ^{208}Pb. Note that cluster radioactivity was experimentally verified in 1984 by Rose and Jones [13] however heavy particle radioactivity (HPR) is still a theoretical concept, which may find experimentally verification in view of advance facilities made available in the recent times.

1.3.3 Spontaneous fission (SF)

Another form of radioactive decay is SF [14] which is found only in heavy and superheavy elements. In order to get stable form, such heavier radioactive systems decay into two fragments and several neutrons, and as a result large amount of energy is released. For the understanding of spontaneous fission, Bohr and Wheeler described the phenomenon of fission [15] on the basis of liquid drop model and established a limit $Z^2/A=48$ for SF, where Z and A are the number of protons and total number of nucleons (proton + neurons) respectively. SF process occurs because

of the competition between short range attractive force which holds together the nucleus, and the electrostatic Coulomb force among protons which cause the oscillations in the nuclear system. These two opposing forces build up a potential barrier, and hence nucleus is distorted from its original shape. If the distortion is small then it emits gamma rays and gets original shape. But if the distortions are large then liquid drop acquire an elongated shape and finally forms a neck. With elongation, repulsive force between protons decreases and surface tension increases and hence the distorted nuclei try to achieve the spherical shape. The atoms having mass greater than 230 undergo via spontaneous fission. The mass of fission fragments decaying via spontaneous fission generally lies in the mass region equal to (A/2)±20, where A is mass of parent nuclei. In our thesis work, an effort is being made to study fission properties like half-life times, probability of formation of decaying clusters, penetration through barrier, and kinetic energy released in SF decay of 'Nobelium' isotopes.

1.4 Excited State Decay mechanisms:

When two stable nuclei are brought together using some external source, an excited compound nucleus (CN) is formed. The idea of CN formation was first suggested by Neil Bohr in 1936 [16]. He proposed a theory which explains the two steps of nuclear reaction which comprises the

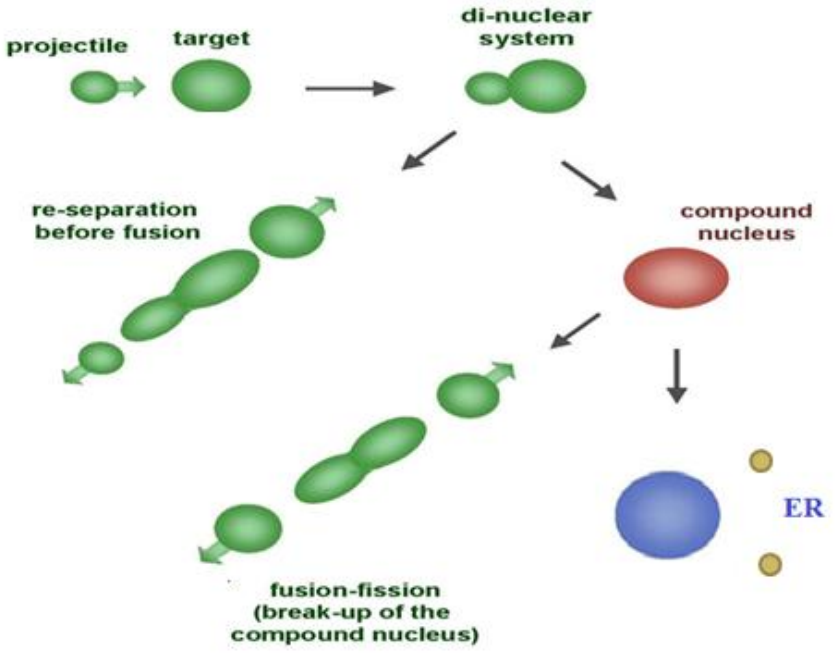

Figure 1.2: *A diagram of different reaction stages observed in compound nucleus (CN) and non-compound nucleus (nCN) processes [17].*

formation of relatively long lived CN and its subsequent decay. Generally, the CN losses its excitation energy by emitting multiple light particles (LPs) and gamma-ray, or immediately undergoes fission. Apart from the formation of CN, the collision of lighter and heavy nuclei leads to a variety of other reaction mechanisms. The non-compound nucleus (nCN) processes are one of them transfer and breakup reactions, quasi fission (QF) and deep inelastic scattering etc. During nCN process, the complete fusion of target and projectile does not take place therefore the interaction time of such processes is relatively short. A schematic view of different reaction stages in the CN and nCN processes is given in figure 1.2.

1.4.1 Evaporation Residue (ER) and Intermediate mass fragments (IMFs) decay mode:

As explained earlier, in order to get the stable state the compound nucleus may emit some light particles and hence loose some extra energy in the process. This mode of decay is known as evaporation residue (ER) [18]. This process is predominant in the compound systems with mass range A_{CN}≈40-100, where fission process contributes minimal. For compound system with mass A_{CN}≈100-200, the intermediate mass fragments (IMFs) [19] with 2≤Z≤10 and 5≤A≤20 appear in the company of heavy mass fragments (HMFs), along with ER and fission. However for the heavier compound system A_{CN}≥200, owing to its instability against centrifugal repulsions the most probable decay mode of the compound nucleus is generally the fission decay [20].

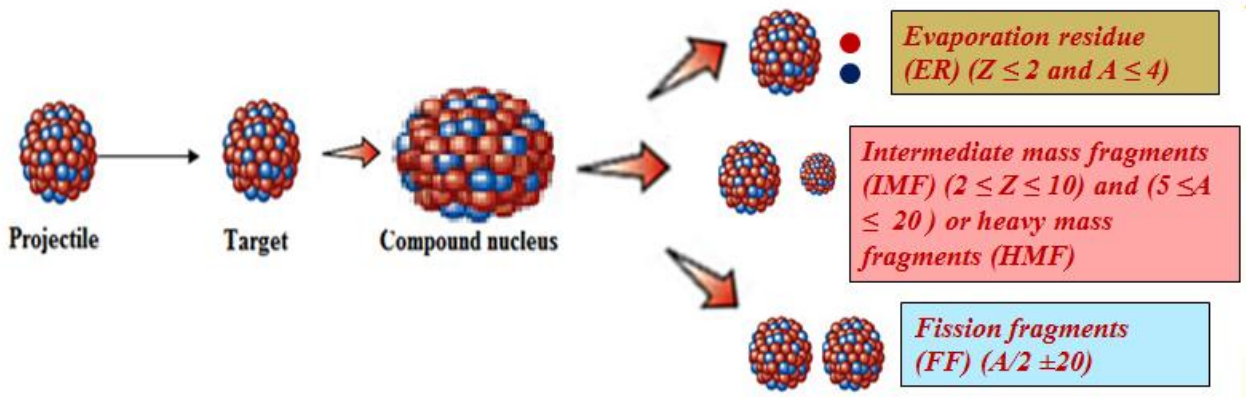

Figure 1.3: *Formation of excited compound nucleus and its decay via different modes like evaporation residue (ER), intermediate mass fragments (IMFs), heavy mass fragments (HMFs) and fission fragments (FF).*

1.4.2 Fusion-Fission Mode:

Seven decades ago, the n-induced fission of ^{235}U was discovered. From that time, the nuclear fission process is important from both fundamental and applied research point of view. Fission can be induced by exciting the compound nucleus by the neutron, proton or other heavy ions. Fusion-fission [21] reactions play an important role in the production of new elements, their further studies and applications, etc. Another important aspect in the study of fusion–fission reactions is the fission fragment mass distribution which has attracted a great deal of attention in the recent years. The fission fragment mass distribution of fissioning nuclei can be symmetric or asymmetric depending upon the nuclear composition, incident energy and deformations involved. The measurement of mass, energy, angular momentum and cross-section of the fission fragments inturn provide important information about the dynamic aspects of fusion-fission process. During fusion-fission process, firstly fusion reaction occur in which a stable nucleus absorb a neutron (or heavy ion) and becomes unstable. In order to achieve stability this excited unstable nucleus (compound nucleus) splits into two lighter fragments. The common example of nuclear fission process is induced fission of Uranium nucleus ${}_0^1n+{}_{92}^{235}U\rightarrow{}_{92}^{236}U^*\rightarrow{}_{56}^{139}Ba+{}_{36}^{94}Kr+3{}_0^1n$, which is also illustrated in figure 1.4.

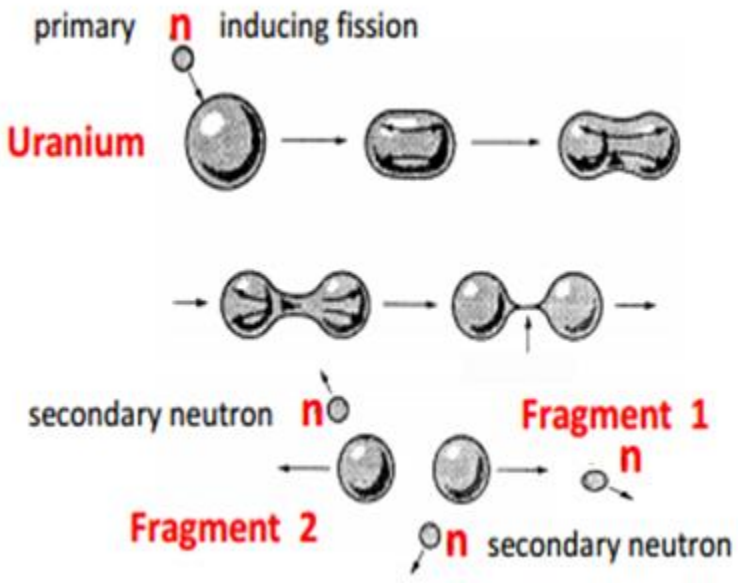

Figure 1.4: *Neutron-induced fission of 'Uranium' nucleus [22].*

In view of this, in the present study an attempt is being made to study the fusion-fission of excited $^{256}No^{*}$ nucleus [23]. In addition to this, a comparative study of spontaneous fission and induced fission of ^{256}No nucleus is also carried out (details are present in chapter 3). In order to do this work, we have applied the quantum mechanical fragmentation theory (QMFT) based formalism known as Dynamical cluster decay model (DCM) and Performed cluster model (PCM). DCM and PCM are respectively applied to address induced fission and spontaneous fission dynamics.

References

[1] M. Pfurtzner and M. Karny, L. V. Grigorenko, K. Riisager, Rev. Mod. Phys. **84** (2012).

[2] Flerov, and Petrjak, phys. Rev., **58**, 89 (1940).

[3] A. Sandulescu and W. Greiner, **55**, 1423-1481(1992).

[4] D.N. Poenaru, R.A. Gherghescu, W. Greiner, Phys. Rev. Lett. **107,** 062503 (2011).

[5] Peter Fong, Phys. Rev. **102**, 434 (1956).

[6] R. K. Gupta, W. Schied and W. Griner, Phys. Rev. Lett. **35**, 353 (1975).

[7] H. Becqueral, C. Reudus **122**, 420 (1896).

[8] Rutherford E. Philos Mag **47**, 109 (1899).

[9] Villard, P., Comptes Rendus **130**, 1010 (1900).

[10] A. Sandulescu, D. N. Poenaru and W. Greiner, Sov. J. Part. Nucl. **11**, 528 (1980).

[11] G. Sawhney, K. Sandhu, M. K. Sharma, and R. K. Gupta, Eur. Phys. J. A **50**, 175 (2014).

[12] K.P. Santosh and B. Priyanka, Nucl. Phys. A **929**, 20-37 (2014).

[13] H. J. Rose and G. A. Jones, Nature (London) **307**, 245 (1984).

[14] Emilio segre, Phys. Rev. **86**, 21 (1952).

[15] N. Bohr and J.A. Wheeler, Phys. Rev., **56**, (1939).

[16] N. Bohr, Nature (Londan) **137**, 344 (1936).

[17] https://www.pinterest.com/pin/545005992379066925/

[18] M. Kaur and M. K. Sharma, Phys. Rev. C **85**, 054605 (2012).

[19] A. K. Dhara, C. Bhattacharaya, S. Bhattacharaya and K. Krishan, Phys. Rev. C **48**, 4 (1993).

[20] M. Kaur, M. K. Sharma and R. K. Gupta, Phys. Rev. C **86**, 064610 (2012).

[21] M.G. Itkis et al., Nucl. Radio. Sci., **3**, 57-61 (2002).

[22] https://ejc2014.sciencesconf.org/conference/ejc2014/pages/goennenwein.pdf

[23] E. V. Prokhorova et al., Nucl. Phys. A **802**, 45-66 (2008).

Chapter 2

Methodology

2.1 Introduction

For understanding the nuclear structure and reaction dynamics of various decay processes, different theoretical approaches are used. The methodology used in present work for the study of spontaneous fission and induced fission is based on Quantum Mechanical fragmentation theory (QMFT) [1-3]. The ground state spontaneous fission decay of unstable nuclei has been investigated using preformed cluster decay model (PCM) [4-9]. Whereas dynamical cluster model (DCM) [10-16], which is reformulation of PCM, gives the relative probability of all decay channels of excited compound nucleus. QMFT is worked out in terms of collective coordinates of mass (and charge) asymmetries $\eta_A = (A_1-A_2)/(A_1+A_2)$ (and $\eta_z = (Z_1-Z_2)/(Z_1+Z_2)$), the relative separation R, multipole deformations $\beta_{\lambda i}$ (λ=2,3,4... and i=1,2), orientations θ_i (i=1,2), azimuthal angle ϕ between the principal planes of the two colliding nuclei and neck parameter (ε). In terms of these collective coordinates and their velocities, the collective Hamiltonian can be written as:

$$H = K(R,\beta,\varepsilon,\eta,\eta_Z;\dot{R},\dot{\beta},\dot{\varepsilon},\dot{\eta},\dot{\eta}_Z) + V(R,\beta,\varepsilon,\eta,\eta_Z)$$

Here β is taken as $\beta_{\lambda 1}$ and $\beta_{\lambda 2}$ with λ=2,3,4...., K refers to the kinetic energy and V to the collective potential energy. For fixed β and ε, the potential V (η, η_z ,R), minimized in the η_z coordinate gives the Schrödinger wave equation, in terms of mass parameters η and relative separation R co-ordinates, as:

$$H(\eta,R)\Psi(\eta,R) = E(\eta,R)\Psi(\eta,R)$$

with the Hamiltonian

$$H(\eta,R) = K(\eta) + K(R) + K(\eta,R) = V(\eta) + V(R) + V(\eta,R)$$

Here, K refers to the kinetic energy and V to the collective potential energy. In decoupled approximation, the Schrödinger equation can be solved using the Hamiltonian:

$$H = \frac{-\hbar^2}{2\sqrt{B_{\eta\eta}}}\frac{\partial}{\partial\eta}\frac{1}{\sqrt{B_{\eta\eta}}} - \frac{\hbar^2}{2\sqrt{B_{RR}}}\frac{\partial}{\partial R}\frac{1}{\sqrt{B_{RR}}}\frac{\partial}{\partial R} + V(\eta) + V(R)$$

For decoupled Hamiltonian, Schrödinger wave equation can be divided for the two coordinates η and R as follows,

$$\left\{\frac{-\hbar^2}{2\sqrt{B_{\eta\eta}}}\frac{\partial}{\partial\eta}\frac{1}{\sqrt{B_{\eta\eta}}}\frac{\partial}{\partial\eta} + V(\eta)\right\}\psi^{\omega}(\eta) = E^{\omega}\psi^{\omega}(\eta)$$

and

$$\left\{\frac{-\hbar^2}{2\sqrt{B_{RR}}}\frac{\partial}{\partial R}\frac{1}{\sqrt{B_{RR}}}\frac{\partial}{\partial R}+V(R,\eta,T)\right\}\psi^{\omega}(R)=E^{\omega}\psi^{\omega}(R)$$

with

$$\psi(\eta,R)=\psi(\eta)\psi(R) \quad \text{and} \quad E=E_{\eta}+E_{R}$$

The states $\psi^{\omega}(\eta)$ are the vibrational states in the potential V (η) and are labelled by the quantum numbers ω = 0, 1, 2, etc.

2.2 The Preformed Cluster-Decay Model (PCM)

The preformed cluster-decay model (PCM) based on the QMFT, assumes that the cluster/fragments are preborn in the parent nuclei with the certain preformation probability P_0 [17]. This methodology relies on collective coordinates (described in previous section), which allow to define decay constant λ and hence decay half-life time $T_{1/2}$ as

$$T_{1/2}=\frac{\ln 2}{\lambda}=\frac{\ln 2}{\nu_0 P P_0}, \qquad \lambda^{PCM} = \nu_0 \, P \, P_0, \tag{1}$$

Here, P_0 is the preformation probability of decaying fragments and P is barrier penetration probability referring to η and R-motion respectively. The impinging frequency υ_0 with which cluster hit the barrier is calculated as

$$\nu_0=\frac{\upsilon}{R_0}=\frac{(2E/\mu)^{1/2}}{R_0} \tag{2}$$

and found to be nearly constant $\approx 10^{-21}s^{-1}$for spontaneous fission decay of No isotopes as listed in table 3.1 ahead. Here in equation (2) R_0 is the radius of parent nucleus, $\mu = [A_1A_2/(A_1+A_2)]m$ being the reduced mass. When both cluster and daughter nuclei are in the ground state then its Q-value is positive and entire Q-value is equal to the kinetic energy which is shared between both the fragments. Q-value is written in terms of kinetic energy of fragments as $Q=E_1+E_2$. Kinetic energy of emitted fragments is written as

$$E_2=\frac{A_1}{A}Q \quad \text{and} \quad E_1 = Q - E_2 \tag{3}$$

The preformation probability $P_0(A_i)$ is the solution of the stationary Schrödinger equation in η, at fixed $R=R_a$

$$\left\{\frac{-\hbar^2}{2\sqrt{B_{\eta\eta}}}\frac{\partial}{\partial\eta}\frac{1}{\sqrt{B_{\eta\eta}}}\frac{\partial}{\partial\eta}+V(R,\eta,T)\right\}\psi^{\omega}(\eta)=E^{\omega}\psi^{\omega}(\eta) \qquad (4)$$

With ω =0,1,2,3,.. referring to ground state (ω =0) and excited state solutions. The solution of this stationary Schrödinger equation is the preformation probability and it is written as

$$P_0(A_i)=\left|\psi(\eta(A_i))\right|^2\sqrt{B_{\eta\eta}}\,\frac{2}{A_{CN}} \qquad \text{where i=1 or 2} \qquad (5)$$

In this work, we are interested only for ground state solution for which ω =0 and T=0. The mass parameter (smooth hydrodynamical masses) $\beta_{\eta\eta}$ are taken from reference [18].

The penetrability P is the WKB integral from R_a to R_b, where R_a and R_b is first and second turning points respectively. The penetrability consists three terms, (i) the penetrability P_i from R_a to R_i, (ii) the de-excitation probability W_i at R_i, and (iii) the penetrability P_b from R_i to R_b, written as

$$P=P_iW_iP_b \qquad (6)$$

According to excitation model of ref. [19], for ground state decays W_i =1, then equation (6) is written as

$$P=P_iP_b \qquad (7)$$

Where P_i and P_b are calculated by WKB approximation as

$$P_i=\exp\left[-\frac{2}{\hbar}\int_{R_a}^{R_i}\{2\mu[V(R)-V(R_i)]\}^{1/2}dR\right], \qquad (8)$$

and

$$P_b=\exp\left[-\frac{2}{\hbar}\int_{R_a}^{R_b}\{2\mu[V(R)-Q]\}^{1/2}dR\right]. \qquad (9)$$

Here R_a is defined as $R_a=C_t+\Delta R$, where $C_t=C_1+C_2$, C_i (i=1,2) is the Sussman's central radius which is related to effective radius R_i, given by

$$C_i = R_i\left(1-\frac{b^2}{R_i^2}\right) \tag{10}$$

and $R_i = 1.28A_i^{2/3} - 0.76 + 0.8A_i^{-1/3}$. ΔR is the only parameter of the model which is known to assimilate the neck-formation effects. The structure information of decaying nuclear system is contained in P_0 via the fragmentation potential V(η,T) at fixed R=R_a is defined as

$$V(\eta, R, \ell, T) = -\sum_{i=1}^{2}\left[B_i\left(A_i, Z_i, \beta_{\lambda i}, T\right)\right] + V_c(R, Z_i, \beta_{\lambda i}, \theta_i, \phi, T) + V_P(R, A_i, \beta_{\lambda i}, \theta_i, \phi, T) + V_\ell(R, A_i, \beta_{\lambda i}, \theta_i, \phi, T)$$

.

Note B_i (A_i,Z_i) are the ground state binding energies taken from Ref. [20]. V_C and V_p represents the repulsive Coulomb and nuclear-proximity potential respectively [21,22].

Apart from above to investigate the fusion-fission of excited compound nucleus the dynamical cluster-decay model (DCM) is used in present work. The DCM for the disintegration of excited composite nucleus ($\ell \neq 0$ and $T \neq 0$), is a reformulation of the PCM (ℓ=0 and T=0). Note that both the theoretical models based on the QMFT. Besides the T and ℓ effects in the disintigration of excited CN, the deformation and orientation effects of the decay products are also taken care in DCM. Note that for ground state spontaneous fission studies, we have used Sussman's central radius [C_i (i=1,2)] of fragments as explained earlier (see eq. (10)). Whereas in the DCM, for decay of excited CN, the first turning point R_a is defined as $R_a=R_t+\Delta R$, where $R_t=R_1+R_2$ and temperature dependent nuclear raddi $R_i(T) = [1.28A_i^{1/3} - 0.76 + 0.8A_i^{-1/3}](1 + 0.0007T^2)$ fm.

References

[1] R. K. Gupta, M. Balasubramanium, R. Kumar, N. Singh, M. Manhas and W. Greiner, J. Phys. G **31**, 631 (2005).

[2] J. Marhun and W. Greiner, Phys. Rev. Lett. **32**, 548 (1974).

[3] R. K. Gupta, W. Schied and W. Griner, Phys. Rev. Lett. **35**, 353 (1975).

[4] S. S. Malik and R. K. Gupta, Phys. Rev. C **39**, 1992 (1989).

[5] S. Kumar and R. K. Gupta, Phys. Rev. C **55**, 218 (1997).

[6] S. K. Arun, R. K. Gupta, B. B. Singh, S. Kanwar, and M. K. Sharma, Phys.Rev. C **79**, 064616 (2009).

[7] S. K. Arun, R. K. Gupta, S. Kanwar, B. B. Singh, and M. K. Sharma, Phys. Rev. C **80**, 034317 (2009).

[8] G. Sawhney, M. K. Sharma, and R. K. Gupta, Phys. Rev. C **83**, 064610 (2011).

[9] R. Kumar and M. K. Sharma, Phys. Rev. C **85**, 054612 (2012).

[10] R. K. Gupta, R. Kumar, N. K. Dhiman, M. Balasubraniam, W. Scheid, and C. Beck, Phys. Rev. C **68**, 014610 (2003).

[11] B. B. Singh, M. K. Sharma, R. K. Gupta, and W. Greiner, Int. J. Mod. Phys. E **15**, 699 (2006).

[12] B. B. Singh, M. K. Sharma, and R. K. Gupta, Phys. Rev. C **77**, 054613 (2008).

[13] S. Kanwar, M. K. Sharma, B. B. Singh, R. K. Gupta, and W. Greiner, Int. J. Mod. Phys. E **18** 1453 (2009).

[14] M. Kaur, R. Kumar, and M. K. Sharma, Phys. Rev. C **85**, 014609 (2012).

[15] N. Grover, G. Kaur and M. K. Sharma, Phys. Rev. C **93**, 014603 (2012).

[16] K. Sandhu, M. K. Sharma, and R. K. Gupta, Phys. Rev. C **85**, 024604 (2012).

[17] R. Blendowske and H. Walliser, Phys. Rev. Lett. **61**, 1930 (1988).

[18] H. Kroger and W. Scheid, J. Phys. G **6**, L85 (1980).

[19] M. Greiner and W. Scheid, J. Phys. G: Nucl. Phys. **12**, L229 (1986).

[20] P. Moller, J. R. Nix, W.D. Myers, and W.J. Swiatecki, At. Data Nucl. Data tables **59**, 185 (1995).

[21] R.K. Gupta, N. Singh, and M. Manhas, Phys. Rev. C 70, 034608 (2004).

[22] R. K. Gupta, S. K. Arun, R. Kumar, and Niyti, Int. Rev. Phys. **2**, 369 (2008).

Chapter 3

Results and Calculations

3.1 Introduction

Knowing that spontaneous fission (SF) play important role in the production and stability of synthesized elements, an attempt has been made to explore the SF of 'Nobelium' isotopes (with mass number varying from A=250 to 262). Ever since the discovery of SF decay from 'Uranium' nucleus [1], the SF has become the considerable subject for investigation of numerous aspects related to nuclear stability. During last 3-4 decades, the fragment mass distributions, total kinetic energies (TKE's), fission half-lives ($T_{1/2}$), and charge (Z) and neutron number (N) of decaying fragments in the decay of SF has been investigated on theoretical as well as experimental front [2-5]. Here, in the present work, the SF half-lives of 'Nobelium' isotopes are calculated by PCM [6,7]. The 'neck-length' parameter (ΔR), is used to fit the recent experimental data [8]. The calculations are performed for spherical choice of fragments and using the Sussman's central radius [9] of nuclei. Moreover, the potential energy surfaces (PES), preformation probability P_0, penetrability P and total kinetic energy (TKE) are explored in view of SF decay process.

Beside this, the most probable fragments decaying via SF are identified with maximum preformation factor. In the last, a comparative study of spontaneous fission and fusion-fission of ^{256}No nucleus is investigated in terms of barrier characteristics, barrier-lowering effects, fragmentation potential and preformation probability for the comprehensive understanding of dynamics is involved. Note that the fission of ^{256}No* formed via ^{48}Ca induced reaction is explored using DCM [10,11].

3.2 Results and discussion

The fragmentation potential $V(A_2)$ in η_A coordinate, is plotted in figure 3.1, for the SF decay of parent ^{250}No, ^{254}No, ^{258}No and ^{262}No nuclei. All calculations have been carried out using best fit value of neck-length parameter for angular momentum ℓ=5ħ, using spherical choice of fragments. Broadly speaking with increase in the mass of parent nucleus, the magnitude of fragmentation potential increases. The behaviour of potential energy surfaces reveal that fragmentation potential is relatively asymmetric for lighter nucleus ^{250}No, and the contribution of asymmetric fragments reduces as one goes from lighter to heavier parent nuclei. The $V(A_2)$

attains minimum value for certain mass region i.e. the fission region for all the spontaneous fissioning nuclei. The vertical arrows are drawn to point out the most probable fragment emitted in the spontaneous

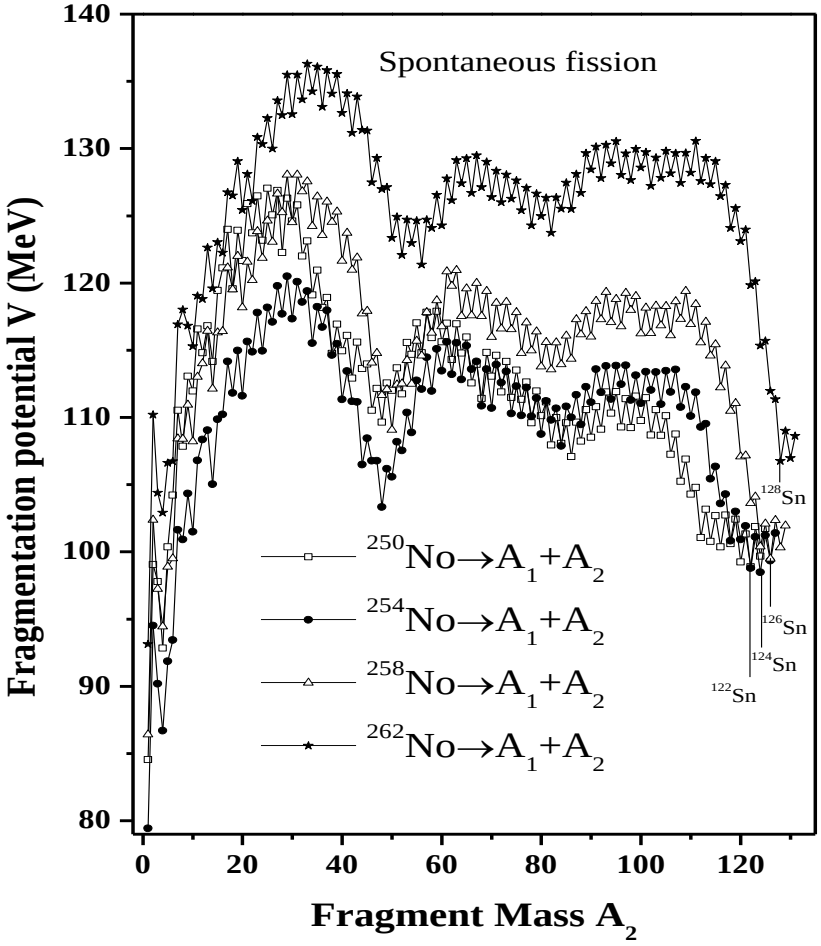

Figure 3.1: *The fragmentation potential $V(A_2)$ plotted for 'Nobelium' isotopes decaying via spontaneous fission. The most probable fission fragments are marked with solid vertical arrows for each parent nuclei.*

fission decay for the considered parent nuclei. The *Sn isotopes with the mass range 122-128 are formed at the bottom of fissioning region and hence Z=50 magicity seem to play an important role here for all the cases we observe strong minima around magic proton number Z_2=50, however the neutron number of most probable emitted element increases with increase in mass

of parent nuclei. Note that for the fragment for which fragmentation potential is minimum posses maximum preformation probability (see figure 3.2) and hence correspond to most probable fragments contribution towards spontaneous fission.

For further verification of above results, figure 3.2 (a to d) shows the preformation factor P_0 for ^{250}No, ^{254}No, ^{258}No and ^{262}No isotopes respectively. PCM is based on collective clusterization process; therefore P_0 gives the relative preformaton probability of all decaying fragments. Arrows are drawn in figure 3.2 to show the best preformed fragment emitted in the spontaneous fission of 'Nobelium' isotopes. One can notice from the figure that the ^{250}No isotope gives the asymmetric mass distribution. However, with increase in mass of the parent nucleus from A=250 to 262, the preformation profile shows a drift from asymmetric to symmetric contribution of fission fragments. It is important to mention here that the P_0 is the spectroscopic factor that provides the significant information about nuclear structure properties of fragments

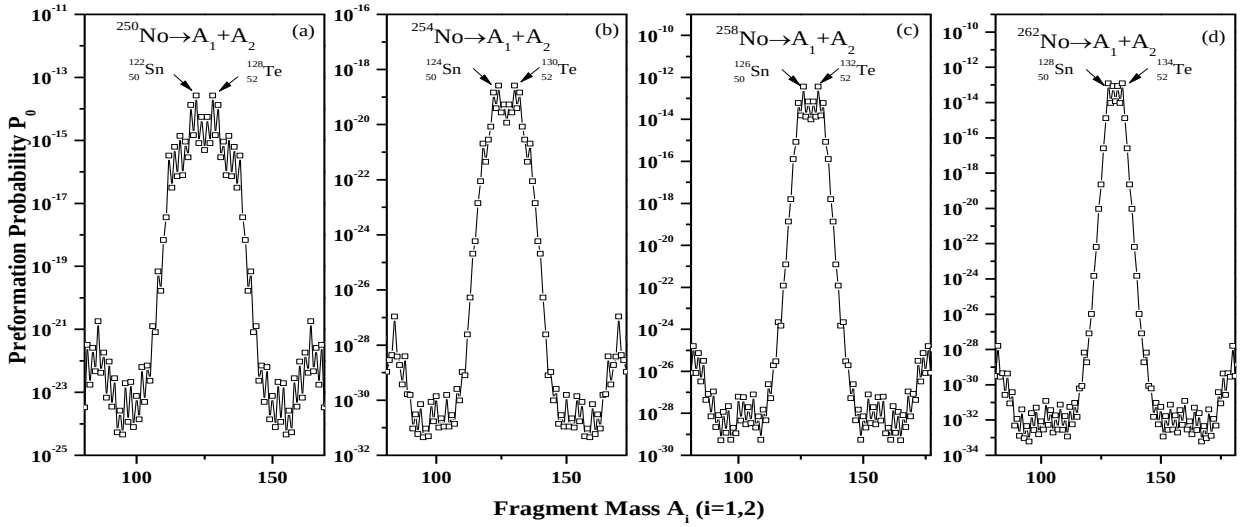

Figure 3.2: *The $P_0(A_i)$ plotted for the decay of (a) ^{250}No, (b) ^{254}No, (c) ^{258}No and (d) ^{262}No spontaneous fissioning nuclei, also showing the presence of shell effects around charge number Z=50 and neutron number N=82.*

formed in parent nucleus. These results of PCM are in accord with the measured experimental [12] observations. The nuclear shell structure effects are clearly visible in preformation probability by its being larger for fragments referring to shell closure around magic number Z=50 and N=82 for all the studied cases.

In order to verify the above results, a comparative analysis of experimental [12] yield and PCM calculated yield has been made here. For this purpose figure 3.3 (a) and (b) show the PCM calculated preformation yield and experimental measured yield respectively, for ^{256}No spontaneous fissioning nuclei. It is evident from figure that the preformation yield depicts

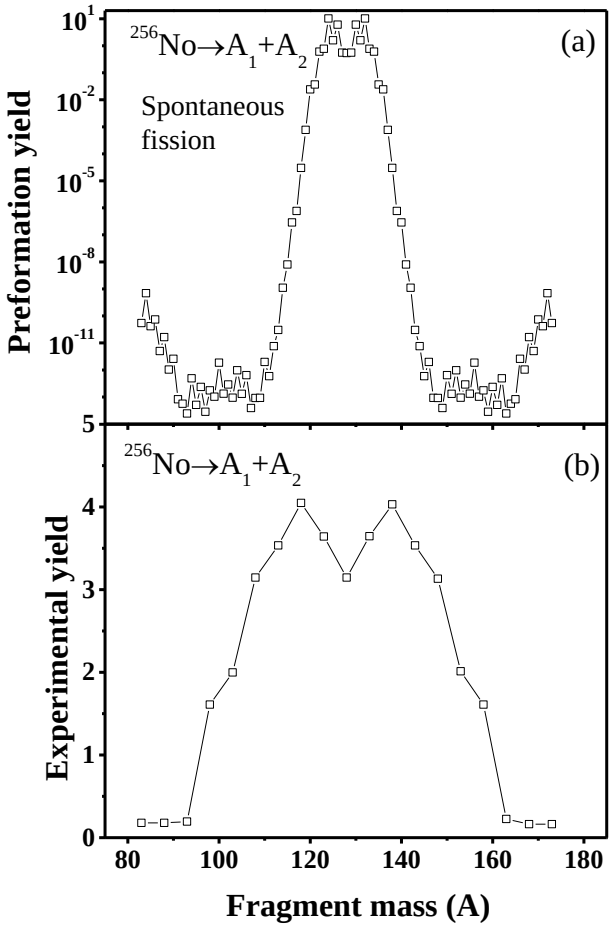

Figure 3.3: *The PCM calculated preformation yield (a) and experimental yield (b) as a function of heavy fragment mass plotted for the SF decay of ^{256}No nuclei.*

asymmetric behaviour for ^{256}No nucleus, which is in line with the behaviour shown by experimental mass yield. Hence, the PCM calculations are found to follows the experimental yields, signifying asymmetric mass distribution for ^{256}No nucleus.

Next, we have calculated the SF half-lives ($T_{1/2}$) of all 'Nobelium isotopes' as listed in Table 3.1. In PCM, the half-life time of decay depends upon formation probability of pre-born fragments P_0, barrier penetration probability P and assault frequency ν_0. All these observables, calculated using best fit value of neck-length parameter 'ΔR', are also presented in Table-3.1. Interestingly, the neck-length parameter shows the decrement with increase in mass of parent nuclei varying from 1.052 fm to -0.64 fm. The assault frequency ν_0 for all the '$^{250-262}$No' isotopes decaying via spontaneous fission remains almost constant $\approx 10^{21} s^{-1}$. Table-I depicts the nice agreement between PCM calculated half-lives and experimental data [8], corresponding to the most probable decaying fragment of each spontaneous fissioning nuclei. As mentioned earlier, for the entire studied No isotopes, the most probable decaying fragments i.e. $^{122-128}$Sn (and their complementary fragments $^{128-132}$Te) in the SF decay lie in the neighbourhood of magic shell closure (Z=50 and N=82).

Table 3.1. *Comparison of PCM calculated spontaneous fission half-lives ($T_{1/2}$) with experimental [6] ones. The other related observables like neck-length parameter (ΔR), preformation probability P_0, penetrability P and assault frequency v_0 are also presented.*

Parent Nuclei	Decaying fragments	ΔR (fm)	Preformation probability (P_0)	Pentrability (P)	Assault Frequency (v_0)	Log$T_{1/2}$ (sec) (PCM)	Log $T_{1/2}$ (sec) (Experimental)
^{250}No	^{122}Sn+^{128}Te	1.052	2.64×10^{-14}	4.27×10^{-7}	2.73×10^{21}	-1.649	-2.301
^{251}No	^{122}Sn+^{129}Te	0.586	1.84×10^{-16}	1.14×10^{-7}	2.72×10^{21}	1.082	1.0
^{252}No	^{122}Sn+^{130}Te	0.165	1.07×10^{-15}	2.42×10^{-8}	2.72×10^{21}	0.991	0.954
^{254}No	^{124}Sn+^{130}Te	0.413	2.62×10^{-19}	3.48×10^{-8}	2.69×10^{21}	4.449	4.459
^{256}No	^{124}Sn+^{132}Te	0.503	1.43×10^{-18}	3.33×10^{-7}	2.69×10^{21}	2.731	2.732
^{257}No	^{125}Sn+^{132}Te	0.511	2.93×10^{-19}	5.26×10^{-7}	2.68×10^{21}	3.224	3.225
^{258}No	^{126}Sn+^{132}Te	-0.26	3.61×10^{-13}	6.13×10^{-7}	2.67×10^{21}	-2.931	-2.92
^{260}No	^{128}Sn+^{132}Te	-0.63	2.16×10^{-15}	5.02×10^{-5}	2.65×10^{21}	-0.261	-0.974
^{262}No	^{128}Sn+^{134}Te	-0.64	1.21×10^{-13}	1.99×10^{-4}	2.65×10^{21}	-4.967	-2.301

Figure 3.4(a) and (b) show variation of logarithm of half-lives ($\log_{10}T_{1/2}$) and preformation probability ($\log_{10}P_0$) corresponding to most probable decaying fragment, as a function of mass of the parent nuclei. It is evident from the figure that half lives Log $T_{1/2}$ shows almost opposite behaviour to the preformation factor (P_0). Figure 3.4 justifies the fact that P_0 imparts significant nuclear structure information in the SF studies of No isotopes.

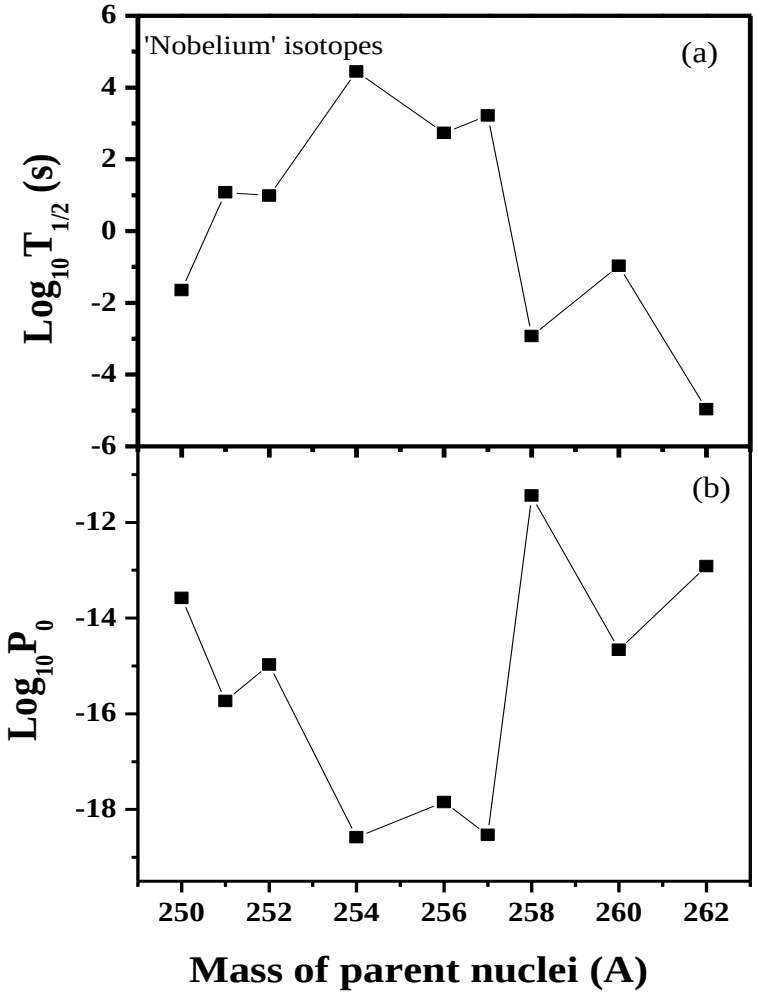

Figure 3. 4(a): *The logarithm of PCM calculated half-lives for* $^{250\text{-}262}$*No spontaneous fissioning nuclei plotted as a function of atomic mass number of parent nuclei and compared with experimental data.* ***(b)*** *Represent the same but for preformation probability* P_0.

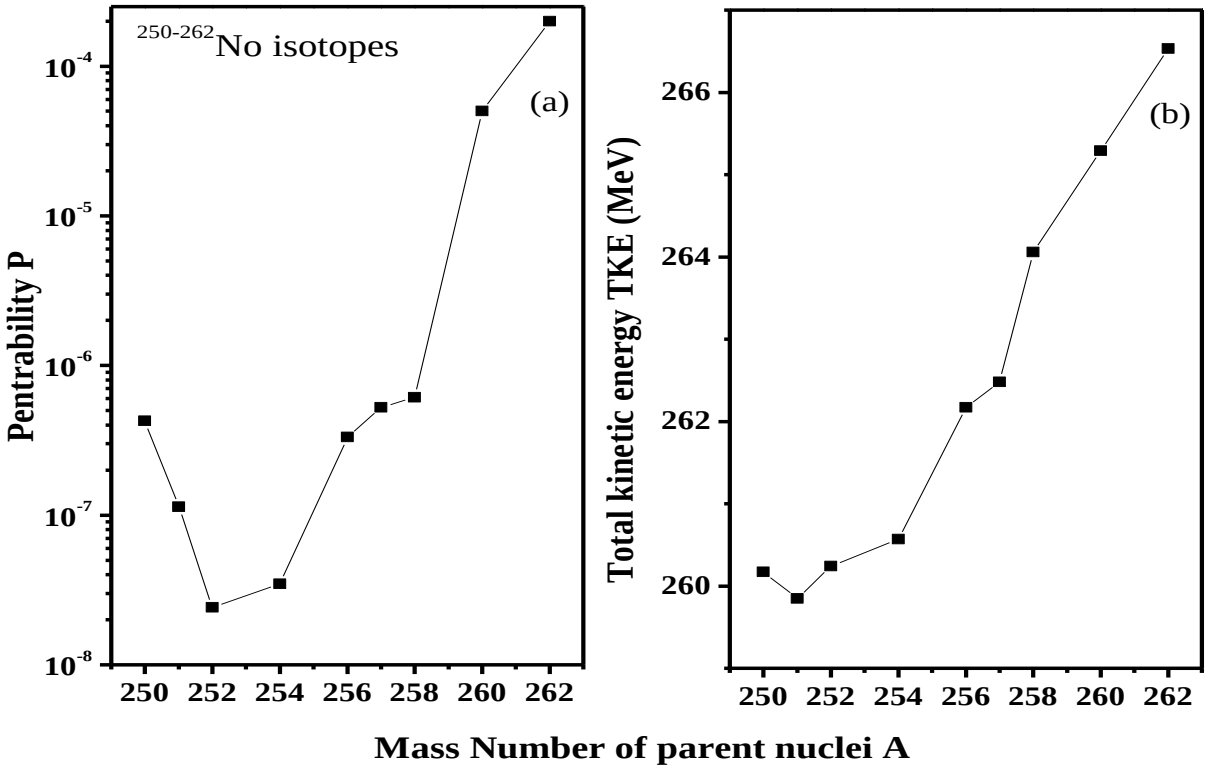

Figure 3.5: *(a) The penetrability P and (b) total kinetic energy (TKE) plotted for various 'Nobelium' spontaneous fissioning nuclei as a function of atomic mass of parent nuclei (A).*

As stated earlier that in PCM the half-life time is combined effect of both P_0 and P. Hence, in figure 3.5(a) the barrier penetration probability is plotted as a function of mass of spontaneous fissioning nuclei. The variation of P calculated for most probable decaying fragments, shows the increment with increase in mass of parent nucleus, that means larger the fragment mass higher the probability of barrier penetration, and similar behaviour of total kinetic energy (TKE) released in the SF decay is depicted as shown in figure 3.5(b). With increase in the mass of the most probable decaying fragments (i.e. ^{122}Sn to ^{128}Sn and ^{128}Te to ^{134}Te), the total kinetic energy of these fragments also show the increment. The penetrability and TKE are relatively higher for ^{250}No nucleus probably due to large magnitude of neck length parameter 'ΔR'.

Next, we have made an attempt to study the comparative analysis of spontaneous fission and induced fission of ^{256}No nucleus. In a recent experiment [13], $^{48}Ca+^{208}Pb\rightarrow^{256}No^{*}$ reaction is studied over a wide range of incident energies. But we have chosen only one lowest energy E_{CN}=13 MeV to explore the induced fission and its comparison with spontaneous fission. The choice of lowest energy is made in the view that comparison is to be carried for spontaneous fission which operates at E=0, T=0 state. Note that we have studied the spontaneous fission and induced fission in the theoretical framework of PCM and DCM respectively. The DCM is used widely to study the disintegration of hot compound nucleus. The measured fission cross-section ($\sigma^{expt.}$=0.045 mb) for $^{256}No^{*}\rightarrow A_1+A_2$ reaction is attained at ΔR=0.332 fm and maximum

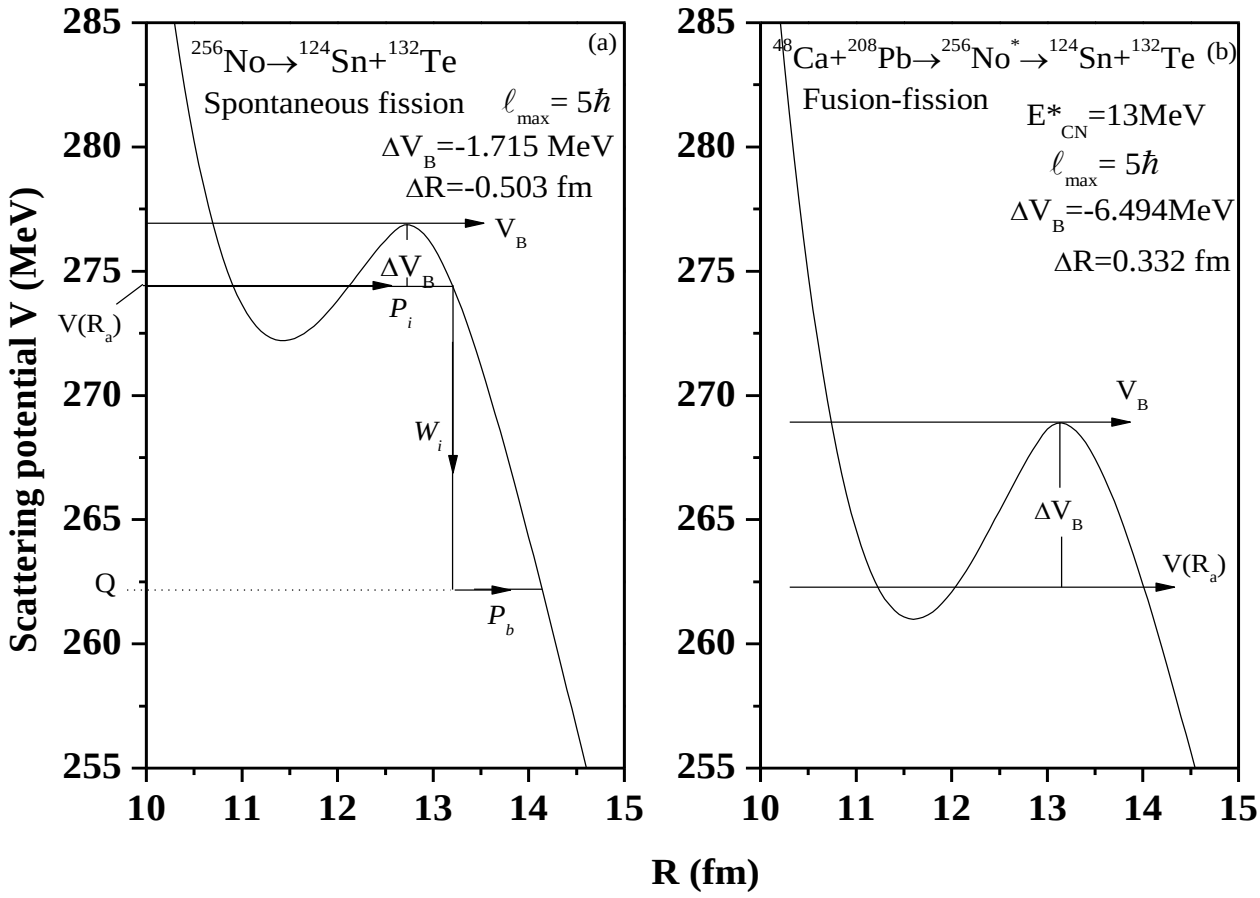

Figure 3.6: *The Scattering potential plotted for the* ***(a)*** *spontaneous fission and* ***(b)*** *fusion-fission of ^{256}No nucleus for the spherical choice of fragments.*

angular momentum ℓ_{max}=108ħ, where the mass of fission fragments (A_2) varies from 116 to 118. All the calculations have been made using spherical choice of fragments. First of all, in figure 3.6, we studied the barrier characteristics of both the processes. Figure 3.6 (a) and (b) shows the scattering potential as a function of inter-nuclear separation R, for spontaneous fission and induced fission at common angular momentum ℓ=5ħ. One can clearly see from the figure that both processes show the different barrier characteristics like barrier heights (V_B), barrier position (R_B) and barrier modification (ΔV_B), thereby effecting the barrier penetration probability P. As shown in figure 3.6(a), the penetration probability P consists of three contributions (i) the penetrability

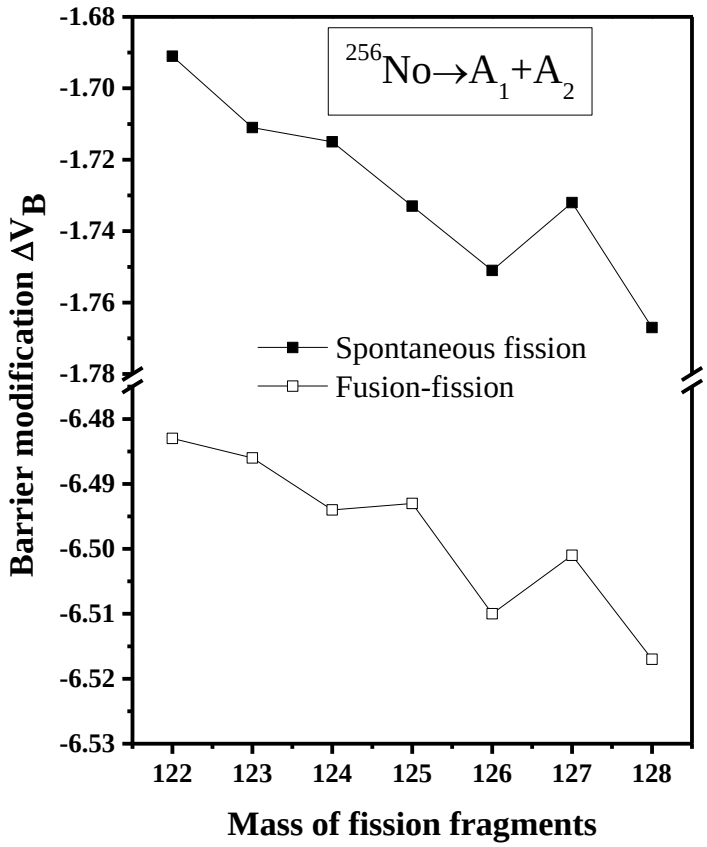

Figure 3.7: *The 'barrier lowering' parameter ΔV_B plotted for spontaneous fission and fusion-fission of ^{256}No nucleus as a function of mass of fission fragments.*

P_i from R_a to R_i, (ii) the (inner) de-excitation probability W_i at R_i, and (iii) the penetrability P_b from R_i to R_b, giving, $P=P_iW_iP_b$. But for the case of fusion-fission it is a single step process as shown in figure 3.6(b). The choice of ΔR's for both processes, seem to suggest that they occur at different time scales. Moreover, as shown in figure 3.6 a higher barrier modification (ΔV_B) (in magnitude) is needed for the case of induced fission process as compared to spontaneous fission decay. Note that 'barrier lowering' effects is intrinsic property of the fitting parameter ΔR, which play important role in addressal of experimental data. For further investigation, figure 3.7 is plotted for comprehensive analysis of 'barrier-modification' parameter as a function of mass of fission fragments for both fusion-fission and spontaneous fission of ^{256}No.

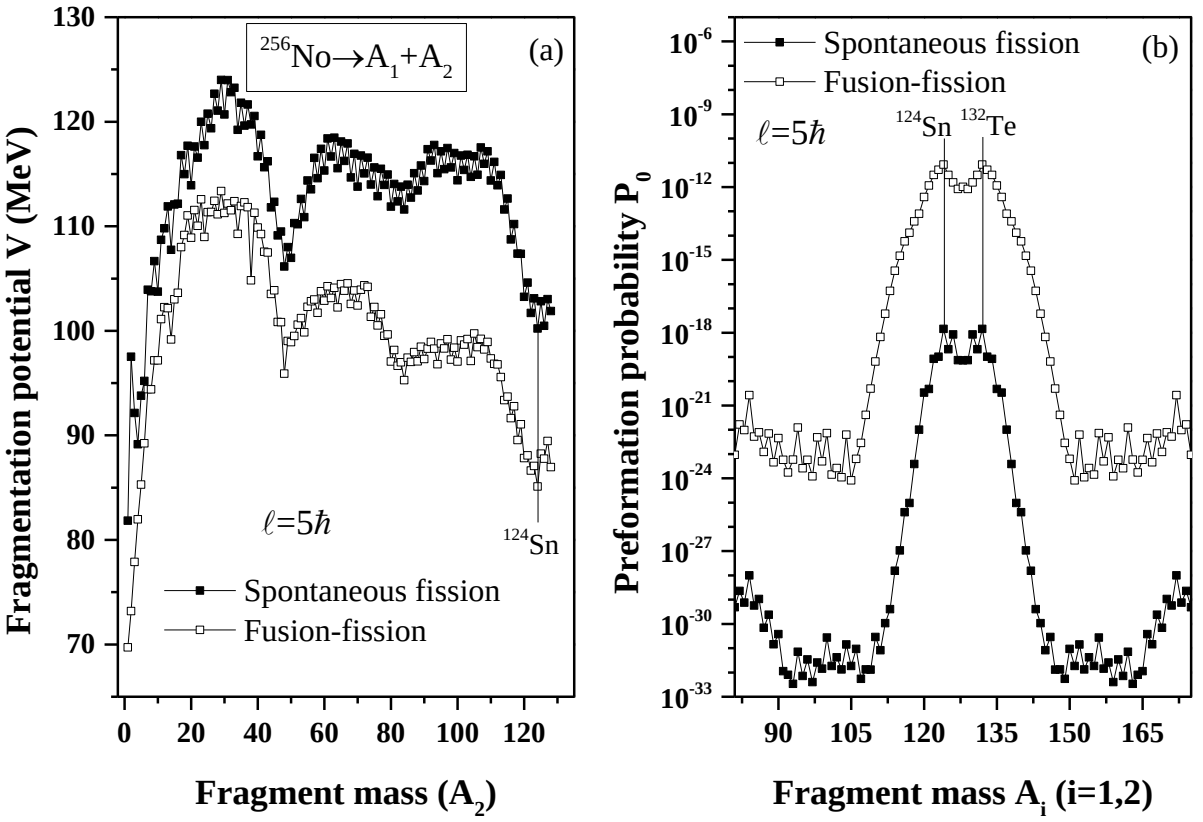

Figure 3.8: (a) *The variation of fragmentation potential $V(A_2)$ plotted for the comparison of spontaneous fission and fusion-fission of ^{256}No nucleus at common angular momentum ℓ=5ħ.* ***(b)*** *Represent the same but for preformation probability P_0.*

From the figure one can see that smaller barrier modification (in magnitude) is required for the spontaneous fission case as compared to fusion-fission process, possibly because fragments are in ground state for SF decay process.

Finally, to see the relative effect of two fission processes, we have plotted the calculated fragmentation potential $V(A_2)$ for SF and fusion-fission in figure 3.8(a) and preformation probability for the same in figure 3.8(b), at common ℓ=5ħ. A minimum in fragmentation potential corresponds to the maximum in preformation probability and vice versa, as illustrated in figure 3.8(a) and (b). It is evident from figure that despite in the change of the magnitude, both the processes show almost similar behaviour in reference to mass distribution and the choice of most probable decaying fragments. The shell effects at (Z=50) and (N=82) are visible in both types of fission processes. This observations suggest that shell closure effects are of equal importance for induced fission as that for spontaneous fission decay. Such observations provide important information for the understanding of stability aspects of spontaneous and induced fission dynamics.

3.3 Summary

Summarizing, in this work, we have analyzed the spontaneous fission (SF) decay of various 'Nobelium' isotopes ($^{250-262}$No) using performed cluster-decay model. We observed that fragmentation potential show relatively asymmetric behaviour for lighter isotopes, this observation is well supported via preformation probability (P_0) analysis. The most probable decaying fragments with maximum preformation factor are identified, and are found to lie in the neighbourhood of shell closure of charge number (Z=50) and neutron number (N=82). These observations of PCM are in line with the experimental results. The behaviour of preformation probability P_0, half-lives ($T_{1/2}$) penetrability P and total kinetic energy (TKE) is analyzed with respect to mass of parent nuclei, which inturn imparts important information regarding the dynamics involved in SF decay process. The calculated half-lives ($T_{1/2}$) of 'Nobelium' spontaneous fissioning nuclei show reasonable agreement with the experimental data. The best fit value of neck-length parameter 'ΔR' show the decrement with increase in the mass of parent nuclei, and vary in the range 1.052 fm to -0.64 fm. The calculated assault frequency v_0 for all the studied nuclei remains almost constant $\approx 10^{21} s^{-1}$.

Finally, the excited state fission decay of $^{256}No^{*}$ nucleus is investigated using DCM. The fragmentation potential (V), prefromation probability (P_0), penetrability (P) and barrier characteristics for fusion-fission decay have been explored and compared with SF dynamics. It is observed that both fission processes show different barrier characteristics, but similar behaviour in reference to the mass distribution and choice of most probable decaying fragments. The nuclear structure shell effects are equally prominent for induced fission as that for ground state decay (spontaneous fission).

It would be of further interest to analyse induced fission data at higher incident energies as well. Preliminary investigation seem to suggest that role of deformations be important for addressal of induced fission cross-section over a energy spread around the Coulomb barrier. Beside this one may explore the role of fragment shapes in view of spontaneous fission as well.

References

[1] Flerov, and Petrjak, Phys. Rev., **58**, 89 (1940).

[2] D.C. Hoffman and M.R. Lane, Radiochim. Acta **70/71**, 135 (1995).

[3] J. P. Balagna et al., Phys. Rev. Lett. **26**, 145 (1971).

[4] E. K. Hulet et al., Phys. Rev. C **40**, 770 (1989).

[5] T. M. Hamilton et al., Phys. Rev. C **46**, 1873 (1992).

[6] S. S. Malik and R. K. Gupta, Phys. Rev. C **39**, 1992 (1989).

[7] S. Kumar and R. K. Gupta, Phys. Rev. C **55**, 218 (1997).

[8] N. E. Holden, D. C. Hoffman, Pure Appl. Chem. **72,** 1525 (2000).

[9] G. Sussmann, Z. Phys. A **274**, 145 (1975).

[10] M. Balasubraniam, R. Kumar, R. K. Gupta, C. Beck, and W. Scheid, J. Phys. G 29, 2703 (2003).

[11] R. K. Gupta, M. Balasubraniam, R. Kumar, D. Singh, and C. Beck, Nucl. Phys. A 738, 479C (2004).

[12] D.C. Hoffman et al., Phys. Rev. C **41**, 2 (1990).

[13] E.V. Prokhorova et al., Nucl. Phys. A **802**, 45-66 (2008).